DiLabio, G.A., Litwinienko, G., Lin, S., Pratt, D.A. & Ingold, K.U. Revised structure for the diphenylaminyl radical: the importance of theory in the assignment of electronic trans…

ARTICLE *in* THE JOURNAL OF PHYSICAL CHEMISTRY A · DECEMBER 2002

Impact Factor: 2.69 · DOI: 10.1021/jp026279i

5 AUTHORS, INCLUDING:

Gino DiLabio
University of British Columbia - Okanagan
124 PUBLICATIONS **4,876** CITATIONS
SEE PROFILE

Grzegorz Litwinienko
University of Warsaw
51 PUBLICATIONS **1,646** CITATIONS
SEE PROFILE

Revised Structure for the Diphenylaminyl Radical: The Importance of Theory in the Assignment of Electronic Transitions in $Ph_2X^{\bullet}$ (X = CH, N) and $PhY^{\bullet}$ (Y = CH_2, NH, O)

Gino A. DiLabio,*,† Grzegorz Litwinienko,*,†,‡ Shuquiong Lin,† Derek A. Pratt,§ and K. U. Ingold†

National Research Council of Canada, 100 Sussex Drive, Ottawa Ontario, Canada K1A 0R6, and the Department of Chemistry, Vanderbilt University, Nashville, Tennessee 37235

Received: June 10, 2002; In Final Form: September 4, 2002

Density functional theory indicates that the minimum energy structure of the diphenylaminyl radical, $Ph_2N^{\bullet}$, has a "staggered" conformation in which the two phenyl rings are twisted relative to each other by an angle, ϕ, of 40°. In this conformation, the aromatic rings are oriented so as to maximize interaction with the unpaired electron while minimizing repulsion between the 2- and 2′-hydrogen atoms. This calculated ground state structure of $Ph_2N^{\bullet}$ differs from that, which has been accepted for the past 15 years, which had the two rings orthogonal ($\phi = 90°$) with one ring conjugating with the nitrogen's lone pair and the other conjugating with the unpaired electron. This structure was based on unexpected differences between the UV−vis absorption spectra of $Ph_2N^{\bullet}$ and the diphenylmethyl radical. However, our calculations indicate that this orthogonal structure lies 3.5 kcal/mol above the global minimum. Further support for the staggered conformation of $Ph_2N^{\bullet}$ is provided by the similarities between absorption transition wavelengths determined theoretically and the experimental absorption bands of $Ph_2N^{\bullet}$ and other diarylaminyl radicals generated by laser flash photolysis. The long wavelength transition of $Ph_2N^{\bullet}$, resulting in a structure that can be represented as $(Ph_2)^{+}N^{-}$, is red-shifted as compared to the related transition from $Ph_2CH^{\bullet}$ to $(Ph_2)^{+}CH^{-}$ due to the electronegativity of the N atom. The absorption bands for $PhCH_2^{\bullet}$, $PhNH^{\bullet}$, and $PhO^{\bullet}$ in the 300−450 nm region are similar in position, which has been taken to indicate that for isoelectronic species the electronic transition energies should be little affected by heteroatom substitution. Our calculations show, however, that these sets of absorption bands arise from different transitions. Therefore, the experimentally similar 300−450 nm absorption bands for these three radicals are fortuitous and do not reflect some common, unifying traits, a fact that further serves to emphasize the importance of theory in the assignment of bands due to electronic transitions.

Introduction

We have recently investigated the effects of substituents on the differences in bond dissociation enthalpies (ΔBDEs) for the N−H bonds in aniline vs 4-substituted anilines, phenothiazine vs 3,7-disubstituted phenothiazines, and diphenylamine vs 4,4′-disubstituted diphenylamines using both theoretical calculations and experimental measurements.[1] The calculated ΔBDEs for both the phenothiazines and the diphenylamines agreed to within 1 kcal/mol with the experimental ΔBDEs determined using the radical equilibrium electron paramagnetic resonance spectroscopy technique.[1] However, the semiempirical method used for geometry optimizations gave a minimum energy structure for diphenylaminyl ($Ph_2N^{\bullet}$) different from that which has been accepted for the past 15 years. Furthermore, this computed structure and the accepted structure could not be reconciled by additional higher level calculations, which were instead found to support the semiempirical $Ph_2N^{\bullet}$ structure. The calculated structure has the two aromatic rings twisted relative to one another with a dihedral angle between the ring planes, ϕ, of about 40 °. The rings are oriented so as to minimize steric interactions between the 2- and 2′-hydrogen atoms while maximizing their conjugative interaction with the unpaired electron. The rings are twisted in opposite directions from the nodal plane of the unpaired electron's orbital (i.e., from the SOMO's nodal plane) at angles, ψ, of about ±20°. The "orthogonal" $Ph_2N^{\bullet}$ structure proposed by Leyva et al.[2] has $\phi = 90°$ with one ring in the SOMO nodal plane ($\psi = 0°$, maximum conjugation with the unpaired electron) and the other perpendicular to this nodal plane ($\psi = 90°$, maximum conjugation with the nitrogen's lone pair of electrons). This structure was proposed because the UV−vis absorption spectra of $Ph_2N^{\bullet}$ and of the isoelectronic diphenylmethyl radical ($Ph_2CH^{\bullet}$) were quite different although they had been expected to be rather similar. Specifically, and as has been known for many years, $Ph_2N^{\bullet}$[3] and ring-substituted diarylaminyls[3a,4] have long wavelength absorptions with λ_{max} in the range of 740−784 nm. An absorption at such long wavelengths is not present in the spectrum of $Ph_2CH^{\bullet}$[5] (nor, for that matter, in the spectra of diarylnitroxides).[6]

As Leyva et al.[2] noted in 1987, "It would be difficult to obtain a reliable prediction for the lowest energy structure of diphenylaminyl from theoretical calculations." Fortunately, this is no longer true. The excellent agreement between our experimental and our calculated ΔBDEs for 4,4′-disubstituted diphenylamines together with our computed optimized $Ph_2N^{\bullet}$ geometry led us to conclude that our $\phi = 40°$, $\psi = \pm 20°$ structure is more likely

* To whom correspondence should be addressed: G.A.D.: Gino.DiLabio@nrc.ca. G.L.: Grzegorz.Litwinienko@nrc.ca.

† National Research Council of Canada.

‡ Permanent address: Warsaw University, Department of Chemistry, Pasteur 1, 02-093 Warsaw, Poland.

§ Vanderbilt University.

10.1021/jp026279i CCC: $22.00
Published on Web 11/12/2002

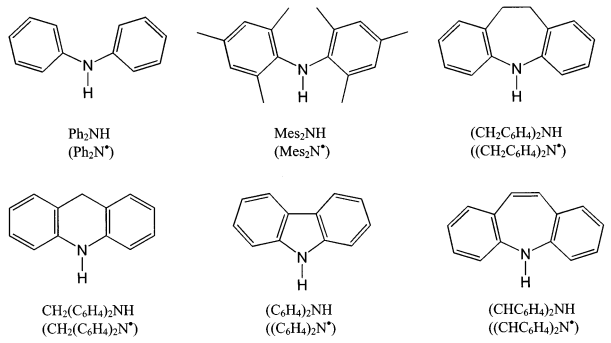

Figure 1. Structures and names of the diarylamines/diarylaminyls studied in this work.

to be correct than the orthogonal structure.[1] Herein, we validate this conclusion by a combination of density functional theory (DFT) calculations of structures and absorption spectra for a number of diarylaminyl radicals combined with experimental measurements of their absorption spectra, including the spectra of radicals derived from three previously unexamined amines, iminodibenzyl, $(CH_2C_6H_4)_2NH$; iminostilbene, $(CHC_6H_4)_2NH$; and dimesitylamine, Mes_2NH. The aminyl radicals were generated from their parent amines by 355 nm laser flash photolysis (LFP) in neat di-*tert*-butyl peroxide, ^{t}BuOO^{t}Bu, or ^{t}BuOO^{t}Bu/benzene, 2:1 v/v:

$$^t\text{BuOO}^t\text{Bu} \xrightarrow{h\nu\ (355\ \text{nm})} 2\,^t\text{BuO}^\bullet \qquad (1)$$

$$^t\text{BuO}^\bullet + \text{Ar}_2\text{NH} \rightarrow {}^t\text{BuOH} + \text{Ar}_2\text{N}^\bullet \qquad (2)$$

The amines (shown in Figure 1) were selected because their molecular architecture dictates that the dihedral angle, ϕ, between the two aromatic ring planes must be 0°, e.g., $(C_6H_4)_2N^\bullet$, slightly greater than 0°, $(CH_2C_6H_4)_2N^\bullet$, and much greater than 0°, $Mes_2N^\bullet$.

Results

LFP. In a typical experiment, 3−5 mM amine was dissolved in carefully deoxygenated neat ^{t}BuOO^{t}Bu or, mainly for solubility reasons, in ^{t}BuOO^{t}Bu/benzene, 2:1 v/v. These solutions were then subjected to 355 nm nanosecond LFP at ambient temperatures, and changes in optical density (OD) were monitored as a function of time at wavelengths ranging from 375 to ca. 800 nm in 10−20 nm intervals. Data were collected at each wavelength from five laser pulses and then averaged. Great care was taken in purifying the amines and keeping them and their solutions out of contact with the air. This was necessary because even trace "impurities" formed by air oxidation of the amine (a particularly facile process in the case of Mes_2NH) gave the solutions a strong absorption at the laser wavelength. Fortunately, none of the pure amines absorbed significantly at 355 nm (at the amine concentrations employed). This is important because the "clean" formation of an aminyl radical via reaction 2 requires that most of the laser's energy, which is absorbed, be absorbed by the ^{t}BuOO^{t}Bu. In this way, the *tert*-butoxyl radicals (^{t}BuO$^\bullet$) are generated only during the laser pulse, i.e., essentially "instantaneously" (reaction 1). Following this pulse, the aminyl radical should "grow-in" with pseudo-first-order kinetics (rate constant, k_{exptl}) and the rate constant for its formation, k_2, can be obtained by monitoring the grow-in at different amine concentrations:

$$k_{exptl} = k_0 + k_2[\text{Ar}_2\text{NH}]$$

TABLE 1: Rate Constants, k_2, for Abstraction of the Amino Hydrogen Atom from Diarylamines by *tert*-Butoxyl Radicals at Ambient Temperatures and Calculated N−H BDEs

amine	λ_{aq} (nm)[a]	$10^{-8}\,k_2$ ($M^{-1}\,s^{-1}$) this work	$10^{-8}\,k_2$ ($M^{-1}\,s^{-1}$) ref 5	N−H BDE[d] (kcal/mol)
Ph_2NH	690	12 ± 2	11 ± 1[b]	84.9
Mes_2NH	400	3.2 ± 0.3	*c*	83.3
$(CH_2C_6H_4)_2NH$	690	12 ± 3	*c*	84.1[e]
$(CHC_6H_4)_2NH$	400	25 ± 3	*c*	79.6
$(C_6H_4)_2NH$	610	1.8 ± 0.4	5.5 ± 1.2	90.3

[a] Acquisition wavelength for kinetic measurements. [b] Another LFP study gives k_2 in a variety of solvents including CCl_4 ($14 \times 10^8\ M^{-1}\ s^{-1}$) and benzene ($15 \times 10^8\ M^{-1}\ s^{-1}$).[7] A less direct competition study gave $k_2 = 23 \times 10^8\ M^{-1}\ s^{-1}$ in benzene.[8] [c] No literature data available. [d] Calculated using the MLM2 model described in ref 9. [e] The calculated N−H BDE for $CH_2(C_6H_4)_2NH$ is 82.1 kcal/mol.

where k_0 represents all first- and pseudo-first-order processes, which might occur in the absence of amine. Quite apart from any intrinsic interest in the k_2 values for different amines, the fact that the absorption grows-in rather than appearing instantaneously after the laser pulse provides confirmation that the absorption spectrum that grows-in is due to the aminyl radical (rather than to some photoexcited species).

Reaction 2 rate constants for the amines studied in the present work are listed in Table 1 together with the available, though very limited, literature data[2,7,8] and with calculated N−H BDEs. A typical grow-in trace, that for the $Mes_2N^\bullet$ radical, is shown in Figure 2.

The absorption spectra of the aminyl radicals are based on the average change in OD (ΔOD) from each of five laser pulses at each of eight well-separated times in the "plateau" region of the grow-in traces (after the grow-in kinetics had been determined using a region of the spectrum where ΔOD following LFP was substantial). In the plateau region, reaction 2 is >90% complete and the aminyl radicals produced do not decay on the time scales of our experiments. Spectra for $Ph_2N^\bullet$, $Mes_2N^\bullet$, and $(CH_2C_6H_4)_2N^\bullet$ are shown in Figure 3 (see also Supporting Information). The only absorption spectra available in the literature for comparison are those for $Ph_2N^\bullet$[2,3b−d] and carbazolyl.[2,3d] Our spectra ($Ph_2N^\bullet$ in Figure 3 and $(C_6H_4)_2N^\bullet$ in the Supporting Information) are in good agreement with the earlier work.

Theoretical Calculations

Minimum energy geometries were calculated for the six aminyl radicals shown in Figure 1 using the (U)B3LYP[11,12] functional with 6-31G(d) basis sets as implemented in the Gaussian 98 program package.[13] In general, these calculations were straightforward and the optimized wave functions had little spin contamination ($S^2 \approx 0.85$). These optimized geometries are summarized in Table 2, which also includes the calculated optimum geometry for the diphenylmethyl radical, $Ph_2CH^\bullet$, and for six nonminimum energy $Ph_2N^\bullet$ structures. All of the structures are provided in Cartesian coordinates as Supporting Information. The transition wavelengths and oscillator strengths for all 12 radicals, computed using time-dependent (TD) DFT ((U)B3LYP/6-31G(d)),[14] are also given in Table 2 together with the experimental absorption maxima measured in this work, supplemented by literature data. Calculated energy changes as a function of the dihedral angle between the two aromatic rings are shown for three initial conformations of $Ph_2N^\bullet$ and $Ph_2CH^\bullet$ in Figure 4.

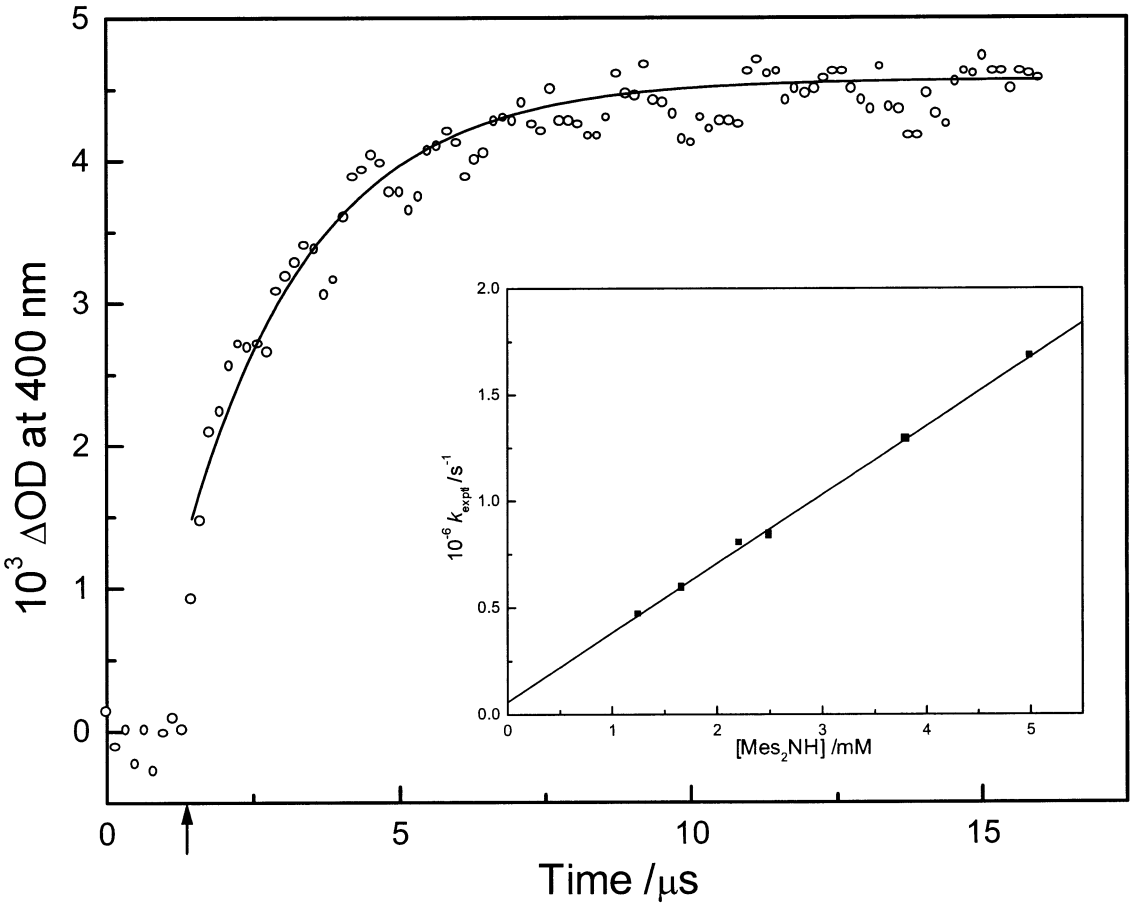

Figure 2. Grow-in trace for $Mes_2N^•$ generated by LFP of a 1.6 mM solution of Mes_2NH in 2:1 v/v ^{t}BuOO^{t}Bu/benzene. The arrow indicates the time at which the laser was fired. The solid line indicates the first-order growth fit of the data to obtain k_{exptl}. The inset shows the linear, least-squares fit of k_{exptl} vs [Mes_2NH] used to obtain the pseudo-first-order rate constant, k_2, for the formation of $Mes_2N^•$.

Discussion

Rate Constants for H-Atom Abstraction from Diarylamines. The noninstantaneous, pseudo-first-order grow-in of the absorptions following LFP of the six Ar_2NH/^{t}BuOO^{t}Bu systems are consistent with the sole occurrence of the chemistry depicted by reactions 1 and 2. That is, the spectra observed at times corresponding to the plateau region of the grow-in traces must be due to the expected $Ar_2N^•$ radicals. The measured values of k_2 are consistent with calculated N−H BDEs (Table 1) except for Mes_2NH, which, for steric reasons, is significantly less reactive than Ph_2NH rather than being comparable. Carbazole is also less reactive than Ph_2NH. This is because the amino hydrogen atom in $(C_6H_4)_2NH$ lies in the aromatic plane and the N−H bond is not, therefore, weakened by resonance stabilization of the incipient radical center by the aromatic π-electron system. Iminodibenzyl, $(CH_2C_6H_4)_2NH$, has the same reactivity as Ph_2NH, which is consistent with their rather similar N−H BDEs, while iminostilbene, $(CHC_6H_4)_2NH$, has the weakest N−H bond and is the most reactive amine.

Transition Wavelengths of Diarylaminyl Radicals. The longest wavelength absorption bands for all of the radicals shown in Table 2 are calculated to involve primarily (85−100%) promotion of an electron from the highest doubly occupied π-molecular orbital (the π_{-1} MO) to the highest semioccupied π-MO (π_0^*). These transitions should therefore be represented as $\pi_0^* \leftarrow \pi_{-1}$.[15] The bands at shorter wavelengths are calculated to involve primarily $\pi_0^* \leftarrow \pi_{-n}$ ($n = 2$, 3, etc.) transitions. For $Ph_2N^•$, $(CH_2C_6H_4)_2N^•$, and $CH_2(C_6H_4)_2N^•$, there is excellent agreement between the calculated $\pi_0^* \leftarrow \pi_{-1}$ wavelengths and

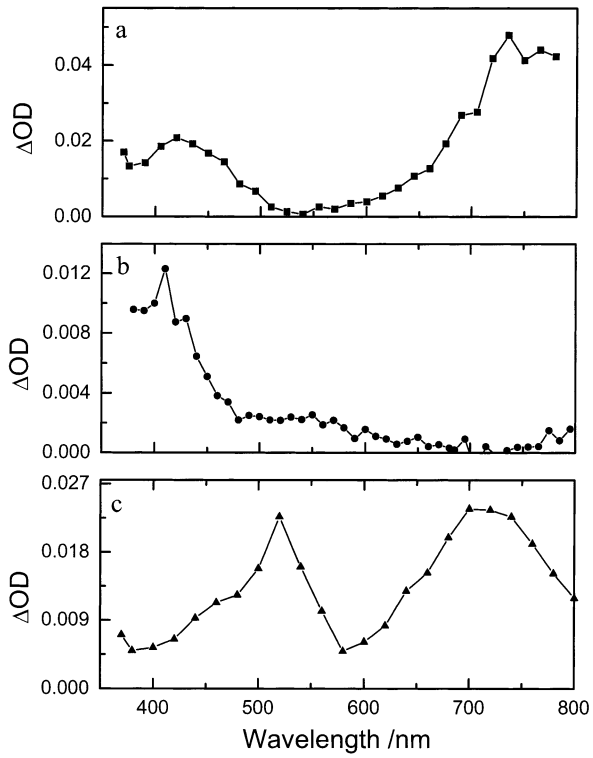

Figure 3. Absorption spectra for aminyl radicals obtained from the average ΔOD from each of five laser pulses at each of eight well-separated times in the "plateau" region of the grow-in traces. (a) $Ph_2N^•$, (b) $Mes_2N^•$, and (c) $(CH_2C_6H_4)_2N^•$.

TABLE 2: Calculated Minimum Energy Geometries, Transition Wavelength (λ_{max}/nm), and Oscillator Strengths (f, in Parentheses) for Six Diarylaminyl Radicals Together with the Same Information for the Diphenylmethyl Radical and for Six Nonminimum Energy $Ph_2N^\bullet$ Structures and the Experimental λ_{max} Values

radical (pt group)	calculations					experiments
	ϕ[a]	ψ[b]	R(C−N•)[c]	θ(CN•C)[d]	λ_{max}[e] (10^3 f)	λ_{max}[f]
$Ph_2N^\bullet$ (C_2)	40	+20, −20	136.8	123.2	750(44), 439(4), 429(1), 398(37)	735,[g] 420[g]
$Mes_2N^\bullet$ (C_2)	68	+34, −34	136.4	126.5	1012(53), 501(9), 474(5), 383(26)	410
$(CH_2C_6H_4)_2N^\bullet$ (C_2)	22	+11, −11	136.4	130.3	724(16), 471(11), 450(7), 441(50)	700, 520
$CH_2(C_6H_4)_2N^\bullet$ (C_{2v})	0	0, 0	136.7	118.6	571(1),[h] 462(5),[h] 460(69), 415(6)	567,[i] 540, 510, 480[i]
$(C_6H_4)_2N^\bullet$ (C_{2v})	0	0, 0	137.7	105.0	954(2), 641(1), 525(79), 409(0)	620,[j] 570, 440[j]
$(CHC_6H_4)_2N^\bullet$ (C_{2v})	0	0, 0	135.8	130.5	734(0),[k] 580(0),[l] 519(13),[m] 430(7)[n]	≤420[o]
$Ph_2CH^\bullet$ (C_2)[p]	40	+20, −20	143.5[q]	130.5[q]	434(1),[r] 383(0), 381(1), 335(17)[s]	523,[t] 336[t]
			$Ph_2N^\bullet$ in constrained geometries			
orthogonal (C_s)	90	0, 90	140.7, 134.5	120.2	911(0), 444(4), 430(1), 364(47)	
orthogonal (C_2)	90	+45, −45	137.6	119.7	859(45), 438(3), 419(3), 377(2)	
planar (C_{2v})	0	0, 0	136.5	130.8	709(0), 473(89), 444(16), 438(5)	
planar (C_{2v})	0	0, 0	136.7[u]	118.6[u]	522(1),[v] 488(98), 460(29), 449(5)	
planar (C_{2v})	0	0, 0	137.7[w]	105.0[w]	511(104), 482(47), 465(4), 397(1)	
$Mes_2N^\bullet$ structure[x] (C_2)	68	+34, −34	136.4[y]	126.5[y]	932(50), 447(3), 436(3), 372(20)[z]	

[a] Angle (in degrees) between the planes of the two aromatic rings. [b] Angles (in degrees) between the aromatic ring planes and the nodal plane of the N 2p singly occupied orbital. [c] C−N• bond length (in pm). [d] CN•C angle (in degrees). [e] The long wavelength band listed first is the lowest energy transition for which the main contribution is the $\pi_0^* \leftarrow \pi_{-1}$ transition unless otherwise noted. The main contributions to the other absorptions are due to $\pi_0^* \leftarrow \pi_{-n}$ (n = 2, 3, etc.) transitions unless otherwise noted. Mixing involving lower energy π levels increases as the wavelength decreases. [f] This work unless otherwise noted. [g] Literature: 760 and 410 nm;[2] 770 and 425 nm.[3d] [h] The 571 nm transition is due to $\pi_0^* \leftarrow \pi_{-3}$. The 462 nm transition is due to $\pi_0^* \leftarrow \pi_{-1}$. [i] Ref 10. [j] Literature: 610 and 560 nm;[2] 617 and 560 nm.[3d] [k] Due to $\pi_1^* \leftarrow \pi_0$. [l] Due to $\pi_0^* \leftarrow \pi_{-2}$. [m] Due to $\pi_0^* \leftarrow \pi_{-1}$. [n] Approximately equal contributions from $\pi_1^* \leftarrow \pi_{-1}/\pi_0^* \leftarrow \pi_{-3}$. [o] See Figure S1 in Supporting Information. [p] As determined from a high-resolution spectroscopy study.[5] [q] Replace N• by C•(H). [r] Approximately equal contributions from $\pi_0^* \leftarrow \pi_{-1}/\pi_1^* \leftarrow \pi_0$. [s] Approximately equal contributions from $\pi_0^* \leftarrow \pi_{-2}/\pi_2^* \leftarrow \pi_0$ (383 nm), $\pi_0^* \leftarrow \pi_{-3}/\pi_3^* \leftarrow \pi_0$ (381 nm), and $\pi_0^* \leftarrow \pi_{-2}/\pi_2^* \leftarrow \pi_0$ (335 nm). [t] Ref 5. [u] Chosen to be the same as in $CH_2(C_6H_4)_2N^\bullet$ but all other structural parameters were optimized. [v] Transition due to $\pi_0^* \leftarrow \pi_{-4}$. [w] Chosen to be the same as in $(C_6H_4)_2N^\bullet$ but all other structural parameters were optimized. [x] This structure was generated by replacing the methyl groups with hydrogen atoms in the optimized $Mes_2N^\bullet$ structure. No further optimization was performed. [y] Chosen to be the same as $Mes_2N^\bullet$. [z] Approximately equal contributions from $\pi_0^* \leftarrow \pi_{-2}/\pi_2^* \leftarrow \pi_0$ (335 nm).

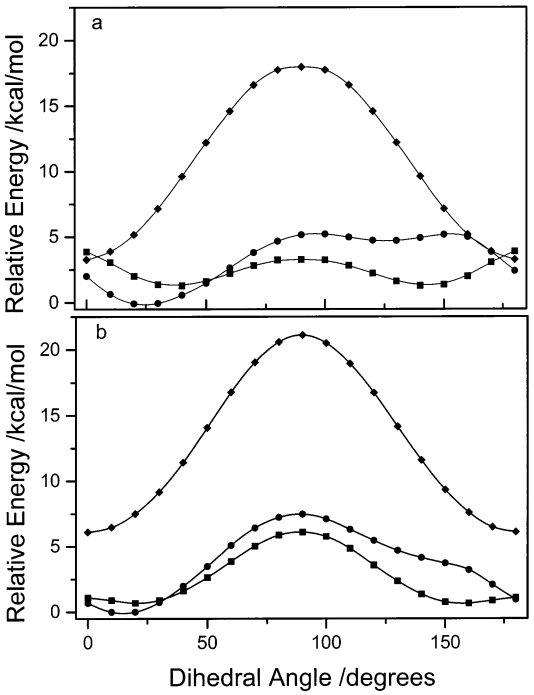

Figure 4. Plots of rotational energy as a function of dihedral angle for three conformations of (a) $Ph_2N^\bullet$ and (b) $Ph_2C^\bullet H$. The dihedral angle, ψ, of one aromatic ring is fixed at ■ = 0°, ● = 20°, and ◆ = 90° with respect to the nodal plane while the second ring is rotated.

the experimental λ_{max} values, the differences in wavelengths being 15, 24, and 4 nm, respectively; see Table 2. For $Mes_2N^\bullet$ and $(C_6H_4)_2N^\bullet$, the calculated longest wavelength transitions at 1 012 and 954 nm, respectively, are outside the spectral detection range of our equipment (limit ca. 800 nm). For $(CHC_6H_4)_2N^\bullet$, we calculate a long wavelength transition with zero intensity, which agrees with the absence of such a peak in the spectrum that we obtained. The calculated shorter wavelength transitions are in reasonable to excellent agreement with experiment (see, e.g., $Ph_2CH^\bullet$ 335 nm (calcd) vs 336 nm (exp)).

Although the calculated transition wavelengths generally agree rather well with experiment, the same cannot be said for the calculated oscillator strengths and observed band intensities. The deficiencies in time-resolved DFT-calculated oscillator strengths have been observed in other systems,[16] and it is well-recognized that they can be misleading in the band assignment process.[16]

The optimized structure of $Ph_2N^\bullet$ has two equivalent aromatic rings, which are twisted 40° (ϕ) relative to one another and ±20° (ψ) out of the nodal plane of the singly occupied orbital; hence, they are not quite maximally conjugated with the unpaired electron.[17]

The excellent agreement between the calculated $\pi_0^* \leftarrow \pi_{-1}$ transition wavelengths and the experimental λ_{max} values for $Ph_2N^\bullet$ and those aminyl radicals necessarily having restricted, nearly planar, or planar geometries, viz., $(CH_2C_6H_4)_2N^\bullet$ and $CH_2(C_6H_4)_2N^\bullet$, gives us confidence in our calculated, slightly nonplanar structure for $Ph_2N^\bullet$. However, to explore the geometric effect on $\pi_0^* \leftarrow \pi_{-1}$ wavelengths, we also carried out calculations on $Ph_2N^\bullet$ held in various nonminimum energy structures (see Table 2). Calculation on the "orthogonal" structure (ϕ = 90°, ψ = 0°, 90°) gave a long wavelength λ_{max} = 911 nm with a very low oscillator strength, a result that is inconsistent with experiment. Keeping ϕ = 90° but conjugating both rings equally with the unpaired electron and nitrogen lone pair by setting ψ = ±45° gave λ_{max} = 859 nm, a result that is also inconsistent with experiment.[17] Turning to planar structures (ϕ = 0°, ψ = 0°, 0°) and minimizing steric repulsion between

the 2- and 2′-hydrogen atoms by allowing both the CNC angle and the C−N bond length to increase yields $\lambda_{max} = 709$ nm, which is slightly farther away from the experimental value of 735 nm than the value calculated for the optimized structure ($\lambda_{max} = 750$ nm; see Table 2). This 709 nm structure is fairly similar to that of $(CH_2C_6H_4)_2N^\bullet$, and not surprisingly, this λ_{max} is close to the calculated (724 nm) and experimental (700 nm) values found for $(CH_2C_6H_4)_2N^\bullet$. When the CNC angle and CN bond lengths for planar $Ph_2N^\bullet$ are constrained to equal those calculated for $CH_2(C_6H_4)_2N^\bullet$ ($\lambda_{max} = 567$ nm), the $\pi_0^* \leftarrow \pi_{-1}$ transition wavelength decreases to 522 nm and has a low oscillator strength and when constrained to the $(C_6H_4)_2N^\bullet$ geometry, this wavelength decreases to 511 nm. Finally, to explore the magnitude of the expected red-shift induced by the six methyl groups in $Mes_2N^\bullet$, calculations were carried out on $Ph_2N^\bullet$ at the $Mes_2N^\bullet$ geometry ($\phi = 68°$, $\psi = \pm 34°$). This causes the $\pi_0^* \leftarrow \pi_{-1}$ transition to decrease in wavelength from 1 012 to 932 nm, only 21 nm larger than the calculated value for the orthogonal structure. Taken in their entirety, the foregoing results overwhelmingly support a minimum energy geometry for the $Ph_2N^\bullet$ radical equal, or certainly close to, that calculated, viz., $\phi = 40°$, $\psi = \pm 20°$.

The geometry of $Ph_2N^\bullet$ is essentially identical to that calculated for $Ph_2CH^\bullet$ (see Table 2). This result is perfectly reasonable provided π-aromatic conjugation with the unpaired electron in $Ph_2N^\bullet$ is significantly more stabilizing than π-aromatic conjugation with the lone pair on the nitrogen. A strong preference for π-aromatic conjugation with the unpaired electron is supported by independent evidence. That is, on the basis of N−H BDEs in $PhNH_2$ and CH_3NH_2,[19] the planar $PhNH^\bullet$ radical can be estimated to be stabilized by 12.0 kcal/mol relative to $CH_3NH^\bullet$ and this must be due to delocalization of the unpaired electron into the aromatic ring. However, the barrier to rotation about the Ph−N bond in $PhNHCH_3$ is only 7.2 kcal/mol.[20,21] Because this barrier must reflect stabilization arising from conjugation of the nitrogen's lone pair with the aromatic π-electrons, it can be seen that conjugation with the lone pair is much less stabilizing than conjugation with the unpaired electron. In $Ph_2N^\bullet$, the two aromatic rings adopt a conformation, which balances maximum interaction with the unpaired electron[23] with minimum steric repulsion between the 2- and 2′-H-atoms.

The energy-minimized structures of $Ph_2N^\bullet$ and $Ph_2CH^\bullet$ differ only in the expected slightly longer Ph−C than Ph−N bond and slightly greater $CC^\bullet HC$ than $CN^\bullet C$ angle. Nevertheless, unlike $Ph_2N^\bullet$, the $Ph_2CH^\bullet$ radical has no long wavelength $\pi_0^* \leftarrow \pi_{-1}$ transition, a spectral difference on which the $Ph_2N^\bullet$ orthogonal structure was largely based.[2] We attribute this difference in the absorption spectra of $Ph_2N^\bullet$ and $Ph_2CH^\bullet$ to the greater electronegativity of nitrogen as compared to carbon. This will make an electronic transition from ground state $Ph_2N^\bullet$ to a state that can be approximately represented by $(Ph_2)^+N^-$ more facile,[15] i.e., red-shifted, as compared with a transition from $Ph_2CH^\bullet$ to $(Ph_2)^+CH^-$.[24] Caution must, therefore, always be exercised when structural assignments are based on similarities and/or differences in the spectra of isoelectronic species unless explicit consideration is given to differences in the electronegativities of the constituent atoms by calculations similar to those described herein.

To explore this matter further, we have applied theory to study the absorption bands of $PhCH_2^\bullet$, $PhNH^\bullet$, and $PhO^\bullet$. In the 300−450 nm range, the bands for these three radicals are similar in position (but not intensity) and therefore appear to be consistent with the prevailing view that for isoelectronic species the electronic transition energies should be little affected by heteroatom substitution.[2] However, TD UB3LYP/6-311+G(d) calculations on the $PhCH_2^\bullet$, $PhNH^\bullet$, and $PhO^\bullet$ radicals show that the bands do not arise from the same transitions, viz., $PhCH_2^\bullet$, 391 ($\pi_0^* \leftarrow \pi_{-1}/\pi_1^* \leftarrow \pi_0$), 365 ($\pi_2^* \leftarrow \pi_0/\pi_0^* \leftarrow \pi_{-2}$), and 324 nm ($\pi_0^* \leftarrow \pi_{-1}/\pi_1^* \leftarrow \pi_0$) (all in reasonable agreement with the experimental values of 448,[25a] 318,[25b] and 305[25b] nm); $PhNH^\bullet$, 539 ($\pi_0^* \leftarrow \pi_{-2}$), 439 ($\pi_0^* \leftarrow \pi_{-1}$), and 360 nm ($\pi_2^* \leftarrow \pi_0/\pi_0^* \leftarrow \pi_{-3}$) (in reasonable agreement with the experimental values of 400 and 308 nm);[25c] $PhO^\bullet$, 1166 (dipole forbidden $\pi_0^* \leftarrow \pi_{-1}$ transition), 533 ($\pi_0^* \leftarrow \pi_{-2}$), and 350 nm ($\pi_0^* \leftarrow \pi_{-3}$) (in reasonable agreement with the experimental values of 1 124, 625, and 397 nm).[26] The very long wavelength, but forbidden, transition for $PhO^\bullet$ is consistent with the expected stability of Ph^+O^-. Therefore, the experimentally similar 300−450 nm patterns of absorption bands for $PhCH_2^\bullet$, $PhNH^\bullet$, and $PhO^\bullet$ are fortuitous and do not reflect some common, unifying traits.

Rotational Energy Surfaces of the Diphenylaminyl and Diphenylmethyl Radicals. To explore further the similarities and differences between $Ph_2N^\bullet$ and $Ph_2CH^\bullet$, the energy changes involved in rotating one phenyl ring about the Ph−N and Ph−C bonds have been calculated while keeping the other phenyl ring at one of three, fixed dihedral angles, ψ, with respect to SOMO's nodal plane. These angles were $\psi = 0$, 20 (ψ for the minimum energy structures), and 90°, and the results are shown in Figure 4. For the cases where the dihedral angle for one ring has been fixed at 20°, both potentials are very flat, which indicates that both $Ph_2N^\bullet$ and $Ph_2CH^\bullet$ will experience large deviations from their minimum energy structures even at room temperature. The barriers to complete rotation of this "free" phenyl group are 5 kcal/mol for $Ph_2N^\bullet$ and 7.5 kcal/mol for $Ph_2CH^\bullet$. The lower barrier in $Ph_2N^\bullet$ is to be expected because at $\psi = 90°$ there is stabilization of this orthogonal ring by conjugative delocalization with the lone pair of electrons on nitrogen. In the cases where ψ for one ring is fixed at 90°, the energy cost of rotating the other ring to $\psi = 90°$ (which breaks its delocalization of the unpaired electron) is 15 kcal/mol for both $Ph_2N^\bullet$ and $Ph_2CH^\bullet$. This energy change is in reasonable agreement with accepted resonance stabilization enthalpies for $PhNH^\bullet$ (12.0 kcal/mol)[19] and for $PhCH_2^\bullet$ (12.2 kcal/mol).[19]

Experimental Section

Method of Calculation. In part, this is described under the Results. Transition wavelengths were calculated using TD (U)-B3LYP[14] with 6-31G(d) basis sets. Additional TD (U)B3LYP/6-311G** calculations on $Ph_2N^\bullet$ and $Mes_2N^\bullet$ produced wavelengths that agreed to within about 5 nm with the results obtained with the smaller basis set. The rotational energy plots shown in Figure 4 are based on the (U)B3LYP/6-31G(d) energies of structures that were partially optimized using the AM1[27] method.

Materials. Spectrograde benzene (OmniSolv) was used as received. ^{t}BuOO^{t}Bu (Aldrich) was passed though neutral alumina before use. Ph_2NH, $(C_6H_4)_2NH$, and $(CH_2C_6H_4)_2NH$ (Aldrich) were recrystallized from hexane (or hexane/ethyl acetate), dried under vacuum, and stored under a nitrogen atmosphere at 4 °C.

Synthesis of Di(2,4,6-trimethylphenyl)nitroxide. Following a literature procedure,[28] 2-bromomesitylene (7.66 mL, 0.05 mol) and magnesium turnings (1.22 g, 0.05 mol) were stirred in a solvent composed of sodium-dried ether (50 mL) and benzene (25 mL). A few crystals of I_2 were added, and the reactants were heated to reflux for 24 h. After they were cooled to room temperature under nitrogen, 2-nitromesitylene (4.13 g, 0.025

mol) in dry ether was added dropwise from a syringe. The solution turned red. Fifteen minutes after the addition was completed, the reaction solution was poured into an aqueous saturated solution of NH_4Cl containing some ice cubes. The aqueous layer was extracted with ether (3×40 mL), and the combined organic solution was dried with anhydrous $MgSO_4$ and concentrated to give the crude dimesityl nitroxide as a red solid. This was thrice recrystallized from MeOH to give 2.5 g of the desired red crystalline product (mp 138−139 °C, Lit.[28] 142−143 °C). The purity and identity of the product were confirmed by thin-layer chromatography (TLC, 15:1 hexane: EtOAc) and high-resolution mass spectroscopy (M + 1: observed $M/Z = 269.1783$ amu, calcd = 269.1780 amu).

Synthesis of Di(2,4,6-trimethylphenyl)amine. An attempted synthesis of this compound from dimesityl nitroxide by the literature procedure[28] was complicated by the amine's extreme air sensitivity. This very rapidly regenerates the nitroxide and makes manipulation of the amine very difficult. The dimesityl nitroxide was therefore reduced directly in the LFP solvent, ^{t}BuOO^{t}Bu. (In a control experiment, this peroxide was found to be stable under the hydrogenation conditions.) Dimesityl nitroxide (107.3 mg, 0.4 mmol) was dissolved in 80 mL of freshly purified ^{t}BuOO^{t}Bu, and platinum(IV) oxide (11.4 mg, 0.05 mmol) was added, followed by hydrogenation for 2 h at room temperature. The solution turned from red to colorless in the first 10 min of hydrogenation. The product solution was transferred to the LFP quartz cuvette under helium. ^{1}H NMR (400 MHz, $CDCl_3$[29]): δ 6.81 (s, 4H), 2.26 (s, 6H), 2.00 (s, 12 H).

LFP. Excitation was provided by a Lumonics HY 750 Nd: YAG laser (third harmonic, 355 nm, 10 ns pulses, 40 mJ/pulse). The transient signals collected by a Tektronix 7912 AD digitizer were transferred to a personal computer that controlled the experiment and provided suitable data processing and storage.

Kinetics. All solutions were deaerated by bubbling with helium for 5 min prior to laser excitation. For each concentration of the parent amine, the mean of at least five transient growth traces of the radical was analyzed by least-squares fitting, on the basis of pseudo-first-order kinetics, to obtain experimental rate constants, k_{exptl}. Values of k_{exptl} plotted vs the parent amine concentration gave straight line fits with R^2 greater than 0.96 in all cases. Full kinetic results are provided in the Supporting Information.

Spectra. All samples were deaerated by passing a stream of helium through the sample before and during the laser experiments. The concentrations of ^{t}BuOO^{t}Bu, benzene (when present), and parent amines were adjusted to obtain absorbance not greater than 0.45 at 355 nm. The concentrations of the parent amines were $[Ph_2NH] = 4.97$ mM, $[(C_6H_4)_2NH] = 5.6$ mM, $[(CH_2C_6H_4)_2NH] = 3.3$ mM, and $[Mes_2NH] = 5.0$ mM. Transient absorption spectra were recorded at 20 °C in a flow system using a 7×7 mm^2 quartz flow-through cell connected with a Teflon line to a sample reservoir. This avoided contamination byproduct build-up. The flow rate was generally 2 mL/min. Transient spectra were collected within the plateau region (see Figure 2) of the kinetic curves.

Acknowledgment. G.L. wishes to thank the Foundation for Polish Science (FNP) for a foreign Postdoctoral Fellowship. D.A.P. thanks Professor N. A. Porter, Vanderbilt University, and NSERC Canada for their support. We also thank Prof. M. S. Platz and the referees for some helpful comments and suggestions.

Supporting Information Available: Kinetic data for the reaction of amines with ^{t}BuOO^{t}Bu. Energies required for the evaluation of N−H BDEs in the arylamines. The fully and partially optimized geometries of the compounds listed in Table 2. The spectra obtained for iminostilbene and for carbazolyl. This material is available free of charge via the Internet at http://pubs.acs.org.

References and Notes

(1) Pratt, D. A.; DiLabio, G. A.; Valgimigli, L.; Pedulli, G. F.; Ingold, K. U. *J. Am. Chem. Soc.* **2002**, *124*, 11085−11092.

(2) Leyva, E.; Platz, M. S.; Niu, B.; Wirz, J. *J. Phys. Chem.* **1987**, *91*, 2293−2298.

(3) Wieland, H. *Annalen* **1911**, *381*, 200−216. (b) Lewis, G. N.; Lipkin, D. *J. Am. Chem. Soc.* **1942**, *64*, 2801−2808. (c) Wiersma, D. A.; Kommandeur, J. *Mol. Phys.* **1967**, *13*, 241−251. (d) Shida, T.; Kira, A. *J. Phys. Chem.* **1969**, *73*, 4315−4320. (e) Johnston, L. J.; Redmond, R. W. *J. Phys. Chem. A* **1997**, *101*, 4660−4665.

(4) See, for example (a) Wieland, H. *Chem. Ber.* **1915**, *48*, 1078−1095. (b) Neugebauer, F. A.; Fischer, P. H. H. *Chem Ber.* **1965**, *98*, 844−850.

(5) Bromberg, A.; Meisel, D. *J. Phys. Chem.* **1985**, *89*, 2507−2513.

(6) Forrester, A. R.; Hay, J. M.; Thomson, R. H. *Organic Chemistry of Stable Free Radicals*; Academic: London, 1968; Chapter 3.

(7) MacFaul, P. A.; Ingold, K. U.; Lusztyk, J. *J. Org. Chem.* **1996**, *61*, 1316−1321.

(8) Lucarini, M.; Pedrielli, P.; Pedulli, G. F.; Valgimigli, L.; Gigmes, D.; Tordo, P. *J. Am. Chem. Soc.* **1999**, *121*, 11546−11553.

(9) Dilabio, G. A.; Pratt, D. A.; LoFaro, A. D.; Wright, J. S. *J. Phys. Chem. A* **1999**, *103*, 1653−1661.

(10) Shida, T.; Kira, A. *Bull. Chem. Soc. Jpn.* **1969**, *42*, 1197−1201.

(11) Becke, A. D. *J. Chem. Phys.* **1993**, *98*, 5648−5652.

(12) Lee, C.; Yang, W.; Parr, R. G. *Phys. Rev. B* **1988**, *37*, 785−789.

(13) Frisch, M. J.; Trucks, G. W.; Schlegel, H. B.; Scuseria, G. E.; Robb, M. A.; Cheeseman, J. R.; Zakrzewski, V. G.; Montgonery, J. A., Jr.; Stratmann, R. E.; Burant, J. C.; Dapprich, S.; Millam, J. M.; Daniels, A. D.; Kudin, K. N.; Strain, M. C.; Farkas, O.; Tomasi, J.; Barone, V.; Cossi, M.; Cammi, R.; Mennucci, B.; Pomelli, C.; Adamo, C.; Clifford, S.; Ochterski, J.; Petersson, G. A.; Ayala, P. Y.; Cui, Q.; Morokuma, K.; Malick, D. K.; Rabuck, A. D.; Raghavachari, K.; Foresman, J. B.; Cioslowski, J.; Ortiz, J. V.; Baboul, A. G.; Stefanov, B. B.; Liu, G.; Liashenko, A.; Piskorz, P.; Komaromi, I.; Gomperts, R.; Martin, R. L.; Fox, D. J.; Keith, T.; Al-Laham, M. A.; Peng, C. Y.; Nanayakkara, A.; Challacombe, M.; Gill, P. M. W.; Johnson, B.; Chen, W.; Wong, M. W.; Andres, J. L.; Gonzalez, C.; Head-Gordon, M.; Replogle, E. S.; Pople, J. A. *Gaussian 98*, revision A.9; Gaussian, Inc.: Pittsburgh, PA, 1998.

(14) Stratmann, R. E.; Scuseria, G. E.; Frisch, M. J. *J. Chem. Phys.* **1998**, *109*, 8218−8224.

(15) This transition can be envisaged as roughly corresponding to the promotion of an aromatic π-electron into the N-2p SOMO, i.e., to the formation of a delocalized aromatic radical cation and a localized nitrogen anion.

(16) See, for example Hirata, S.; Lee, T. J.; Head-Gordon, M. *J. Chem. Phys.* **1999**, *111*, 8904−8912.

(17) The possibility that one (or both) of the aromatic rings in $Ph_2N^\bullet$ is (are) preferentially conjugated with the lone pair on nitrogen rather than with the unpaired electron has been considered and rejected on the basis of substituents effects on the ESR spectra of ring-substituted diphenylaminyls. See Danen, W. C.; Neugebauer, F. A. *Angew. Chem., Int. Ed. Engl.* **1975**, *14*, 783−789.

(18) Note that all structures with $\phi = 90°$ will have equal energy irrespective of their ψ angles.

(19) See Table 2 in Ingold, K. U.; Wright, J. S. *J. Chem. Educ.* **2000**, *77*, 1062−1064.

(20) Lunazzi, L.; Magagnoli, C.; Guerra, M.; Macciantelli, D. *Tetrahedron Lett.* **1979**, 3031−3032. (b) Lunazzi, L.; Magagnoli, C.; Macciantelli, D. *J. Chem. Soc., Perkin Trans. 2* **1980**, 1704−1707.

(21) $\Delta G^\ddagger = 7.24 \pm 0.02$ kcal/mol, $\Delta H^\ddagger = 7.6 \pm 0.2$ kcal/mol, $\Delta S^\ddagger = 2 \pm 1.5$ cal/mol/K.[20a] The inversion barrier for aniline is much lower (1.6 kcal/mol).[22]

(22) Brand, J. C. D.; Williams, D. R.; Cook, T. J. *J. Mol. Spectrosc.* **1966**, *20*, 359−380.

(23) This interaction energy will follow a $\cos^2 \psi$ relation and $\cos^2 20° = 0.88$, i.e., only 12% below the maximum of 1.0 at $\psi = 0°$. It is also worth noting that on the basis of the ESR coupling constants, it has been calculated that the unpaired electron in $Ph_2N^\bullet$ is delocalized into the phenyl groups to the extent of ca. 60%; see Neugebauer, F. A.; Bamberger, S. *Angew. Chem., Int. Ed. Engl.* **1971**, *10*, 71.

(24) Although the frequency of the long wavelength absorption band of $Ph_2N^{\bullet}$ might be expected to change in more polar solvents (in view of the dipolar nature of the excited state), no change was detected in 70% ^{t}BuOO^{t}Bu/30% CH_3CN.

(25) Porter, G.; Ward, B. *J. Chim. Phys.* **1964**, *61*, 1517−1522. (b) Porter, G.; Strachan, E. *Spectrochim. Acta* **1958**, *12*, 299−304. (c) Land, E. J.; Porter, G. *Trans. Faraday Soc.* **1963**, *59*, 2027−2037.

(26) Radziszewski, J. G.; Gil, M.; Gorski, A.; Spanget-Larsen, J.; Waluk, J.; Mróz, B. J. *J. Chem. Phys.* **2001**, *115*, 9733−9738.

(27) Dewar, M. J. S.; Zoebisch, E. G.; Healy, E. F.; Stewart, J. J. P. *J. Am. Chem. Soc.* **1985**, *107*, 3902−3909.

(28) Neugebauer, F. A.; Bamberger, S. *Chem. Ber.* **1974**, *107*, 2362−2382.

(29) By reduction in $CDCl_3$ in an NMR tube.